ILL Number: 36559426

183743

ARTICLE ODYSSEY

Lender Information: CFI
Call #:
QC276 .H5
Location: **Compact Stacks**

Journal Title: High temperature.

Volume: 26 **Issue:**
Month/Year: 1988**Pages:** 170-175

Article Author:

Article Title: .I. Gorokhovskii, V.P. Elovikov, P.L. Lizunov, S.A. Pantyukhin; An Induction Method of Determining Conduction-Zone Size in a Vacuum Arc

Fax: (406) 994-4117
Ariel: 153.90.170.65
Odyssey: 153.90.170.11

Billing: **Exempt**

CFI TN: 338864

Borrower Information: MZF

Lending String: MCA,*CFI,SCT,YDM,LRT

Patron: Gorokhovsky, Vladimir

From: CSU Fullerton – CFI
Library-Interlibrary Loan; P.O. Box 4150; Fullerton, CA 92834
(714) 278-2637; libraryill@fullerton.edu

To: Montana State Unversity, Bozeman -MZF
M.S.U. Libraries - ILL
1 Renne Library
Bozeman, MT 59717-0332

MZF TN: 183743

LITERATURE CITED

1. G. E. Norman, L. S. Polak, P. I. Sopin, and G. A. Sorokin, in: Synthesizing Compounds in a Plasma Containing Hydrocarbons [in Russian], Nauka, Moscow (1985), p. 33.
2. E. P. Lee, Phys. Fludis, 21, No. 8, 1327 (1978).
3. E. Lauer, R. Briggs, T. Fessenden, et al., Phys. Fluids, 21, No. 8, 1344 (1978).
4. K. G. Gureev, V. O. Zolotarev, and S. D. Stolbetsov, Fiz. Plazmy, 10, No. 6, 1027 (1984).
5. E. R. Nadezhdin and G. A. Sorokin, Fiz. Plazmy, 9, No. 5, 989 (1983).
6. L. E. Aranchuk, V. D. Vikharev, V. V. Gorev, et al., Pis'ma Zh. Eksp. Teor. Fiz., 36, No. 7, 331 (1982).
7. P. I. Sopin, Teplofiz. Vys. Temp., 23, No. 2, 235 (1985).
8. S. I. Andreev, V. L. Bychkov, O. A. Gordeev, and I. L. Klepando, Fiz. Plazmy, 11, No. 9, 1134 (1985).
9. S. Brown, Elementary Processes in Gas-Discharge Plasmas [Russian translation], Gosatomizdat, Moscow (1961).

AN INDUCTION METHOD OF DETERMINING CONDUCTION-ZONE SIZE IN A VACUUM ARC

V. I. Gorokhovskii, V. P. Elovikov, P. L. Lizunov, and S. A. Pantyukhin

UDC 533.9:537.523.5

An induction method has been used to determine the size of the conduction zone in a vacuum arc discharge as a function of longitudinal magnetic field strength. The arc column here is a conducting channel contained in a relatively cold low-conductivity sheath consisting of excited cathode-material atoms. The arc column as a whole and the conducting part expand by diffusion, where the diffusion coefficient is inversely proportional to the external longitudinal magnetic field. The results are compared with spectral and probe data.

The conductivity distribution over the arc column is one of the major parameters for a vacuum arc. A difference from a high-pressure arc is that there is no agreed view even on the simple topic of whether there is a conducting channel in a vacuum arc. It is difficult to apply probe methods to the conductivity distribution in a vacuum arc because the probe material has poor resistance in the central region, and also because conducting films grow rapidly on the probe in a vacuum arc metal plasma. Also, an arc in a magnetic field results in current transport asymmetry and then probe dimensions comparable with the arc column size may introduce large errors difficult to monitor. It is therefore important to use contactless methods.

A widely used method for measuring conductivity distributions under stationary conditions [1, 2] and in pulse discharges [3] is induction, in which the parameters of a tuned circuit are dependent on the effects on the coil enclosing the discharge, which is influenced by the conductivity distribution over the plasma channel. The method is most effective in determining conduction-zone dimensions, because the parameters such as the inductance, quality factor, and impedance are dependent on those dimensions ($U \sim D_\sigma^n$, where $n = 2$-4, U is the measuring-instrument reading, and D is conduction-zone diameter), as there is a marked skin effect [3]. We have determined the size of the high-conductivity zone in a vacuum arc as a function of the discharge parameters by that method.

We examined the conductivity distribution with the Fig. 1 apparatus. The arc was struck along the axis of the vacuum chamber 1 between the water-cooled cathode 2 (truncated cone) and copper anode 3 (water-cooled disk) coaxial with the cathode. The electrodes were separated by 100 mm. The conical cathode (angle at vertex 20°) ensured that the arc spot was stabilized at the end [4]. The working end was 5 mm in diameter, so the discharge axis was

Superhard Materials Institute, Ukrainian Academy of Sciences. Translated from Teplofizika Vysokikh Temperatur, Vol. 26, No. 2, pp. 239-245, March-April, 1988. Original article submitted September 25, 1986.

 0018-151X/88/2602-0170$12.50

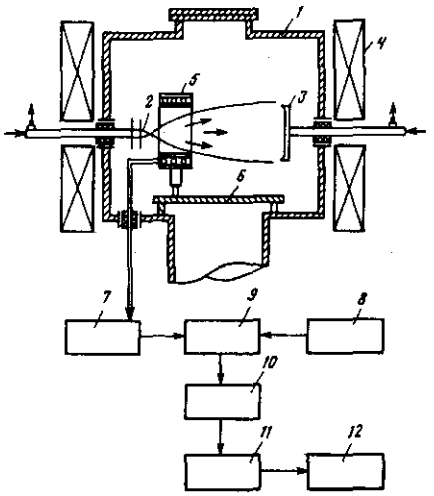

Fig. 1

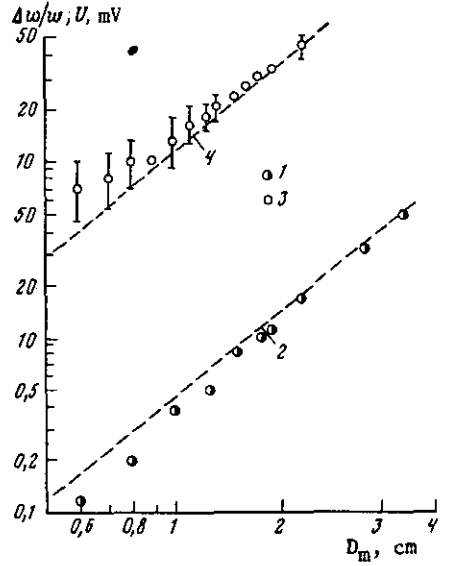

Fig. 2

Fig. 1. The apparatus.

Fig. 2. The $\Delta\omega/\omega = f(D_m)$ and $U = f(D_m)$ relations: 1) $\Delta\omega/\omega$ from (5); 2) from (7); 3) U from experiment; 4) approximation of (8).

closely localized. The arc was initiated by a high-voltage pulse applied to an additional electrode. The arc was supplied from a VD-30IU welding rectifier. An electronic circuit connected the arc for a set period in the range 0.7-4 sec with an error of not more than 0.01 sec, which provided reproducible conditions. The magnetic system 4 provided an axial field in a cylindrical volume up to 200 mm in diameter, homogeneity better than 5%.

A vacuum of $p \leqslant 10^{-3}$ Pa was maintained during the measurements. An induction sensor was used, which included the inductance coil 5 having three copper turns, diameter $D_c = 60 \pm 10$ mm, which exceeded the diameter of the luminous zone in the discharge, which was $D_0 \approx 50 \pm 10$ mm for the minimal field $H_0 = 1.6$ kA/m. The coil was insulated from the plasma by being sealed into an annular gap between two coaxial silica cylinders. The current leads to the coils were through seals on the chamber flange. The coil was adjusted along the axis by means of the rod 6. To exclude coil heating effects, the discharge burning time during the measurements was restricted to 1 sec by the circuit.

The block diagram (Fig. 1) includes the measurement oscillator 7 and heterodyne 8 tuned to 10 MHz, the mixer 9 with 500 kHz passband, the emitter follower 10, and a frequency-sensitive detector 11, which had adjustable sensitivity. The recorder 12 was a millivoltmeter. The capacitance, inductance, and resistance in the connecting cables were minimized by making them as short as possible, so the electronic unit was attached directly to the vacuum chamber flange. The frequency deviation was measured by the beat method. In it, the deviation in the oscillator frequency was determined from the change in the difference between the frequency it provided and that of a stable reference generator (heterodyne). The changes in difference frequency were measured by passing the voltages from the two oscillators to a mixer, whose output was a voltage at the difference frequency, which passed to the emitter follower and then to the frequency-sensitive detector. The recorder readings are proportional to the difference-frequency change.

The resonant frequency is given by

$$\omega_c = 1/(2\pi\sqrt{L_c C}), \tag{1}$$

where C is the capacitance and L_c is the inductance in the measurement coil containing the conducting core. One should distinguish between the strong and weak skin effects in interpreting these induction results [3, 5]; these differ in the magnitude of the parameter

$$\alpha = \frac{2\delta}{D_m} = \frac{1}{D_m}\sqrt{\frac{2}{\pi\sigma\omega\mu_0}}, \tag{2}$$

where δ is the skin depth and D_m is the diameter of the conducting core introduced into the measurement coil (with axial symmetry), while σ is the core conductivity. For $\alpha \ll 1$ (strong skin effect), the method enables one to measure the core dimensions. There is an error associated with the finite penetration depth, which is of the order of α. For $\alpha \gg 1$ (weak skin effect), one can in principle determine the core conductivity, and by varying the frequency, one can determine the conductivity distribution from the change in penetration depth. We have measured the conduction-zone dimensions with a frequency chosen to produce the strong skin effect in the vacuum arc plasma. To estimate α, the conductivity was determined from Spitzer's formula

$$\sigma = 1.93 \cdot 10^4 \frac{T_e^{3/2}}{(\bar{z} \ln \Lambda)}, \tag{3}$$

where $\bar{z}$ is the mean ion charge, T_e electron temperature in eV, Λ the Coulomb logarithm, and σ in $\Omega^{-1} \cdot m^{-1}$.

A vacuum arc in copper vapor gives $\bar{z} = 1.4$-1.7 [6], $T_e = 2$-4 eV [7, 8]. If we take $\bar{z} = 1.4$, $T_e = 3$ eV, $\ln \Lambda = 8$, then (3) gives $\sigma \approx 9000\ \Omega^{-1} \cdot m^{-1}$. Then we specify the characteristic arc diameter as $D \approx 3$ cm (with $H \to 0$) and $\omega = 10$ MHz, which from (2) gives $\alpha \approx 0.1 \ll 1$, i.e., the strong skin effect condition is obeyed.

The arc shrinks as the field strengthens, and the strong condition is violated at a certain H. However, in that case for $\alpha \geq 1$, the method enables one to judge the zone size at least qualitatively, because the circuit parameters have a more marked dependence on the zone size than on the conductivity for the weak effect ($U \sim \sigma D_\sigma^n$, $n = 2$-4) [3, 5, 9].

Copper rods were used to calibrate the sensor for the strong effect. A conducting rod along the axis with the strong effect reduces the inductance by an amount proportional to the field energy in the rod volume. Then the relation between inductance and rod diameter is approximately

$$L_{cm}/L_c \simeq 1 - \varkappa (D_m/D_c)^2, \tag{4}$$

where L_c and L_{cm} are the inductance without the core and with the core material, while D_c and D_m are the diameters of the coil and core.

One can consider (4) as the first terms in an expansion of L_{cm}/L_c in powers of the normalized diameter $\bar{D}_m = D_m/D_c$. For an infinitely long coil, $\varkappa = 1$ [9]. When the core is introduced, the resonant freqency changes by

$$\Delta\omega/\omega_0 = 1 - \sqrt{L_c/L}_m, \tag{5}$$

where ω_0 is the frequency without the core.

One uses (4) to write (5) as

$$\Delta\omega/\omega_0 \simeq 1 - 1/\sqrt{1 - \varkappa \bar{D}_m^2}. \tag{6}$$

For $D_m \ll 1$, (6) gives

$$\Delta\omega/\omega_0 \simeq \varkappa \bar{D}_m^2/2. \tag{7}$$

Figure 2 shows $\Delta\omega/\omega = f(D_m)$, where $\Delta\omega/\omega$ is derived from (5) and the inductance was measured with an E12-1 instrument. The results fit (7) well for $\varkappa = 0.9$. Figure 2 also shows $U = f(D_m)$, where $U(D_m) \sim \Delta\omega$, together with the quadratic approximation

$$U = 11.4 D_m^2, \tag{8}$$

where U is in mV and D_m is in cm.

Formulas (5) and (7) interpret the measurements reliably. There are deviations at small core diameters because the reading is very much dependent on the rod centering. The readings obtained with various cores can be used as calibration ones for determining arc conduction-zone sizes.

A qualitative check on the diameter measurements requires comparison with ones made by some other method. We determine the diameter of the luminous zone for this purpose by means of an MRS-1 spectrum recorder having a time resolution of 1-100 μsec.

The MRS-1 gave the luminous-zone diameter without the broadening associated with transverse shifts. The high-conduction zone diameter was derived by the spectral method from the transverse distributions for the atomic and ionic copper line intensities [10]. The horizontal arc was imaged on the entrance slit of an STE-1 spectrograph, and photographic plates

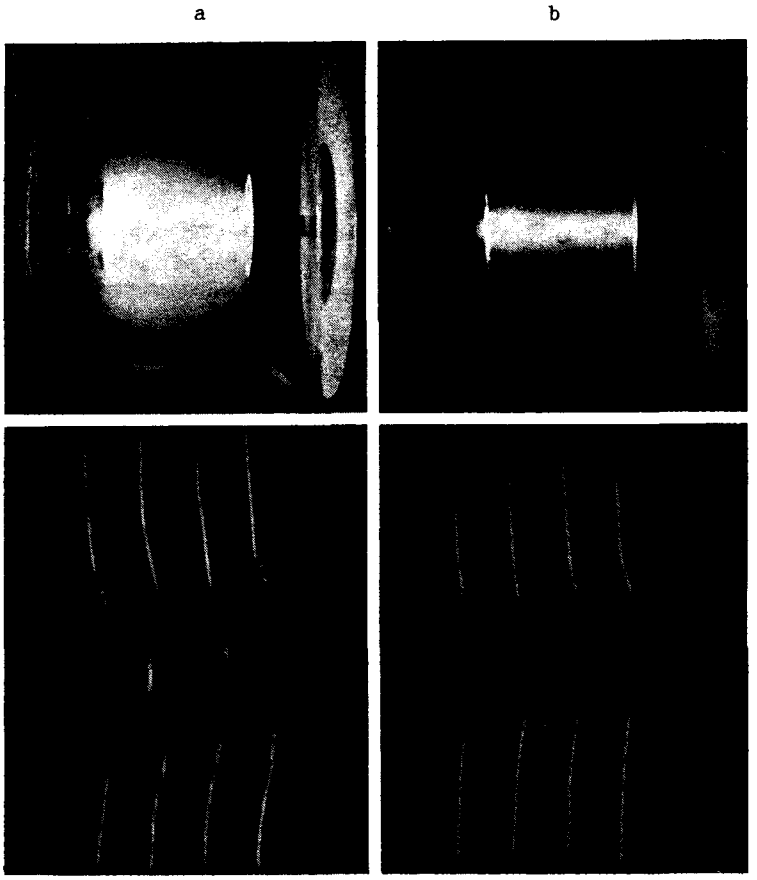

Fig. 3. Photograph and MRS recordings for a vacuum arc operating at 96 A, sweep period 20 μsec: a) H = 1.6 kA/m; b) 44.

recorded the image at various wavelengths. The characteristic curves were determined from the iron spectrum recorded with an IG-3 spark generator through a nine-step attenuator. An MF-1 microphotometer recorded the densities, from which the characteristic curves were constructed, and we then determined the intensities for the Cu I 249.2 nm, Cu II 248.9 nm, and Cu III 248.2 nm lines. We had first checked that the plasma was optically transparent at those wavelengths, for which we measured the intensity from a strip tungsten lamp, beam transmitted transverse to the axis. No absorption was detected. The radial intensity distribution was derived by computer from an inverted Abel equation by the [11] method. Also, a planar Langmuir probe was used to record the ion-current density distribution at saturation in the arc column (the probe potential was equal to the cathode one).

Figure 3 shows photographs and MRS recordings for two axial fields. As the field increases, the plasma jet is compressed, and the diffuse peripheral emission occurring as background is accompanied by a brightly emitting axial zone.

Figure 4 shows the normalized diameter for the high-conduction zone $\overline{D} = D/D_0$ as derived by the induction and probe methods (from the half-width of the radial saturation ion current distribution) as a function of $\overline{H} = H/H_0$, where D_0 is the conduction-zone diameter for $H_0 \approx$ 1.6 kA/m; it also shows the characteristic luminous-zone diameters: the integral-emission zone in the visible region derived from the MRS recordings and the zones for the copper atom and ion lines. The integral emission zone coincides approximately with the luminous zone for the copper atoms but is much wider than the luminosity zones for the singly and doubly ionized copper ones. The MRS recordings give an emission zone somewhat narrower than the atomic luminosity one from the spectral measurements, because the fast recording has high time resolution by comparison with photography, where the luminous zones are averaged over the transverse pulsations. Also, the diameter of the luminosity zone for the atoms D_a is much less dependent on the field than is that for the copper ions. The doubly charged copper ions give a diameter much less than that for the singly charged ones, with the latter approximately coincident with the D_σ found by the induction method, which agrees with conclusions

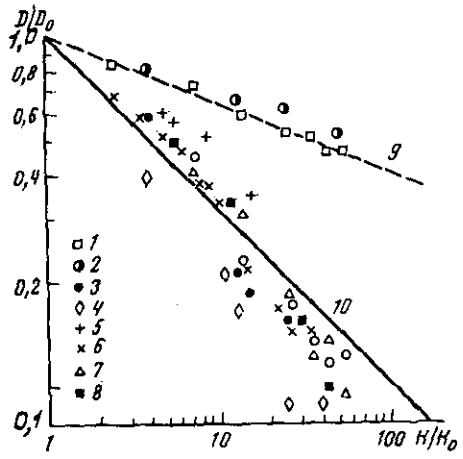

Fig. 4. Effects of field strength (H_0 = 1.6 kA/m) on the diameters of the conduction and luminosity zones [points are from experiment: 1) MRS recordings; 2) Cu I 249.2 nm intensity; 3) Cu II 248.9; 4) Cu III 248.2; 5) probe measurements; 6) induction sensor at 60 A; 7) 80 A; 8) 100 A; the straight lines are approximations: 9) $D/D_0 = (H/H_0)^{-0.2}$; 10) $D/D_0 = (H/H_0)^{-0.5}$].

[7] on determining conduction-zone dimensions in cathode jets from ion-luminosity zone sizes. At high fields, and for diameters in plasma jets comparable with the skin layer thickness, the strong skin-layer approximation does not apply, and then calibration on copper cores can give an error of the order of the conducting-region size itself. The normalized diameters as functions of field can be fitted closely to

$$\bar{D}_i = \bar{H}^n \tag{9}$$

with n = 0.2 for copper atom luminosity zones, n = 0.5 for the conduction zone measured by the sensor, and n = 0.7 for the doubly charged copper ion luminosity zone.

The arc current also has only a slight effect on the conduction-zone diameter (D_σ increases by5% as the current increases from 60 to 100 A).

Standard results on plasma propagation in a longitudinal field [12] suggest that the plasma diffuses transverse to the field with a certain diffusion coefficient dependent on the field and in general on the other discharge parameters: $D = D(H, T_e, I_a, \ldots)$.

The plasma moves with a certain constant speed $v_\parallel$ lengthwise ($v_\parallel \approx 10^4$ m/sec for copper [8, 13]), with this speed acquired by the ions mainly near the cathode, while in the arc column, where the accelerating field is weak, it hardly alters. Then the conduction-zone radius at any point x along the axis is

$$r_\sigma = r_{\sigma 0} + \beta\sqrt{Dx/v_\parallel}, \tag{10}$$

where $r_{\sigma 0}$ is the cathode spot radius (initial conduction-zone radius) and β is a certain coefficient.

We consider a section of the discharge fairly remote from the cathode, i.e., $r_\sigma \gg r_{\sigma 0}$, where (9) gives

$$D = \frac{v_\parallel}{\beta^2 x} r_\sigma^2. \tag{11}$$

If $v_\parallel$ is only slightly affected by the field, (9) and (11) give

$$D \sim H^{-2n}. \tag{12}$$

As n = 0.5 for a conduction zone, that zone expands with a diffusion coefficient inversely proportional to the field, which is characteristic of anomalous Bohm diffusion. Then (10) gives the diffusion coefficient from the measurements for $\beta \approx 1$ and $v_\parallel \approx 10^4$ m/sec as $D \approx 10$-100 m^2/sec, which agrees as to order of magnitude with the Bohm diffusion coefficient. Anomalous diffusion occurs here because there are dissipative and magnetohydrodynamic instabilities [14].

The behavior of the doubly charged copper-ion luminosity zone diameter implies that the diffusion coefficient for a plasma at the axis is closer to the classical result ($D \sim H^2$) than at the periphery, which can be explained if we assume that the plasma flow in the axial zone is laminar, while the instabilities arise near the conduction-zone boundary, where there are temperature and density gradients, which agrees with [15-17].

The results also imply that ions with high charges concentrate in regions with higher plasma density, which is characteristic of equilibrium distributions for ions of various

types in cylindrical plasma columns in axial fields [18]. On the other hand, the field has little effect in the luminosity zone for the copper atoms, where the charged-particle concentration is small.

The diameter of the luminous and conducting zone increases with the current for the following reason. The speed of the coherent motion decreases as the arc current increases [8, 13], which from (10) should increase the column diameter at a given section.

We are indebted to B. A. Uryukov and Yu. L. Ladikov-Roev for interest and valuable advice.

LITERATURE CITED

1. W. N. Blackman, in: Ion, Plasma, and Arc Rocket Engines [Russian translation], Gosatomizdat, Moscow (1961), p. 227
2. Olson and Lary, PNI, 33, No. 12, 41 (1962).
3. A. F. Aleksandrov, A. T. Savichev, and I. B. Timofeev, in: Low-Temperature Plasma Diagnosis [in Russian], Nauka, Moscow (1979), p. 105.
4. I. G. Kesaev, Cathode Processes in an Electric Arc [in Russian], Nauka, Moscow (1968).
5. L. P. Poberezhskii, Teplofiz. Vys. Temp., 7, No. 1, 25 (1969).
6. I. I. Aksenov and V. M. Khoroshikh, Particle Fluxes and Mass Transfer in a Vacuum Arc (Review) [in Russian], TsNIIatominform., Moscow (1984).
7. V. I. Rakhovskii, Izv. Sib. Otd. Akad. Nauk SSSR, Ser. Tekh. Nauk, 3, No. 1, 11 (1975).
8. M. P. Zektser and S. A. Lyubimov, Zh. Tekh. Fiz., 49, No. 1, 3 (1979).
9. G. Burkhart and G. Rapp, in: Low-Temperature Plasmas [Russian translation], Mir, Moscow (1967), p. 362.
10. N. I. Fal'kovskii, Abstracts for the Fifth All-Union Conference on Low-Temperature Plasma Generators [in Russian], Vol. 2, Nauka, Novosibirsk (1972), p. 113.
11. Yu. E. Voskoboinikov, N. G. Preobrazhenskii, and A. I. Sedel'nikov, Measurement-Data Processing in Molecular Gas Dynamics [in Russian], Nauka, Novosibirsk (1984).
12. A. A. Gurin, L. L. Pasechnik, and A. S. Popovich, Plasma Diffusion in Magnetic Fields [in Russian], Naukova Dumka, Kiev (1979).
13. J. Lafferty (ed.), Vacuum Arcs [Russian translation], Mir, Moscow (1982), p. 432.
14. B. B. Kadomtsev, "Plasma turbulence," in: Plasma Theory Topics [in Russian], Issue 4, Atomizdat, Moscow (1964).
15. R. V. Neidigh and C. H. Weaver, Proc. II Conf. PUAE, Vol. 31, United Nations, Geneva (1958), p. 315.
16. A. V. Zharinov, At. Energ., 7, No. 3, 215 (1959).
17. A. V. Zharinov, At. Energ., 10, No. 4, 368 (1961).
18. V. M. Zhdanov, Transport Phenomena in Multicomponent Plasmas [in Russian], Énergoizdat, Moscow (1982).